SANDIA REPORT

SAND2003-4291
Unlimited Release
Printed December 2003

Analysis of Nano-scale Films and Particles

E. David Reedy, Jr.

Prepared by
Sandia National Laboratories
Albuquerque, New Mexico 87185 and Livermore, California 94550

Sandia is a multiprogram laboratory operated by Sandia Corporation,
a Lockheed Martin Company, for the United States Department of Energy's
National Nuclear Security Administration under Contract DE-AC04-94AL85000.

Issued by Sandia National Laboratories, operated for the United States Department of Energy by Sandia Corporation.

Available to DOE and DOE contractors from
U.S. Department of Energy
Office of Scientific and Technical Information
P.O. Box 62
Oak Ridge, TN 37831

Telephone: (865)576-8401
Facsimile: (865)576-5728
E-Mail: reports@adonis.osti.gov
Online ordering: http://www.doe.gov/bridge

Available to the public from
U.S. Department of Commerce
National Technical Information Service
5285 Port Royal Rd
Springfield, VA 22161

Telephone: (800)553-6847
Facsimile: (703)605-6900
E-Mail: orders@ntis.fedworld.gov
Online order: http://www.ntis.gov/help/ordermethods.asp?loc=7-4-0#online

SAND2003-4291
Unlimited Release
Printed December 2003

Analysis of Nano-scale Films and Particles

E. David Reedy, Jr.
Material Mechanics Department
Sandia National Laboratories
P. O. Box 5800 MS-0893
Albuquerque, NM 87185-0893

Abstract

This one-year feasibility study was aimed at developing finite element modeling capabilities for simulating nano-scale tests. This work focused on methods to model: 1) the adhesion of a particle to a substrate, and 2) the delamination of a thin film from a substrate. Adhesion was modeled as a normal attractive force that depends on the distance between opposing material surfaces while delamination simulations used a cohesive zone model. Both of these surface interaction models had been implemented in a beta version of the three-dimensional, transient dynamics, PRESTO finite element code, and the present study verified that implementation. Numerous illustrative calculations have been performed using these models, and when possible comparisons were made with existing solutions. These capabilities are now available in PRESTO version 1.07.

Introduction

Nano-scale films and structured materials are of increasing interest in emerging technologies of importance to Sandia. For instance hard tribological coatings, with a thickness of 10-50 nm, are being considered for Si-MEMS and Ni-LIGA structures. One critical aspect of successfully deploying such materials is an assessment of their performance and durability. There are a number of potentially useful test methods to evaluate nano-scale films and particles. For example, stressed over-layers can induce ~10-nm thick films to delaminate from a substrate, and a nanoscratch tester can push nano-clusters off the substrate to which they adhere. Unfortunately, fundamental material parameters are not measured directly in such tests; rather detailed mechanics-based models must be used in conjunction with the experimental data to deduce the desired properties. The deformation and failures generated in nano-scale tests are typically quite complex, and adhesion and elastic deformation often dominate material response (yielding normally occurs only at very high stress-levels at the nano-scale). In this one-year LDRD feasibility study, methods for modeling nano-scale tests were investigated.

Adhesion is modeled as a normal attractive force that depends on the distance between opposing material surfaces while delamination is simulated using a cohesive zone model [1]. Both of these surface interaction models had been implemented in a beta version of the three-dimensional, transient dynamics, PRESTO finite element code [2] and are now available in PRESTO version 1.07. Contact capabilities in PRESTO are provided by ACME (*Algorithms for Contact in a Multiphysics Environment* [3]), and cohesive zone and adhesion models were implemented via ACME. During the past year, the PRESTO implementation of the adhesion and cohesive zone models has been verified, and numerous illustrative calculations were performed using these models. In all of these calculations, the materials were idealized as linear elastic. Elastic deformation often dominates in nanostructured materials since conventional dislocation-based plastic deformation mechanisms are suppressed at this length scale. Presented below are the results of two illustrative calculations. In one calculation, the force required to pull a 25-nm radius polysilicon cylinder off of a thick polysilicon substrate is determined as a function of adhesion energy. In another calculation, a 100 nm thick tungsten strip is pulled off of a silicon substrate. These 2-D plane strain problems were selected because they highlight phenomena that are important in modeling nano-scale tests while still being sufficiently idealized to permit a comparison with existing, closed-formed solutions.

Illustrative Examples

Polysilicon cylinder on a thick polysilicon substrate

The 2-D, plane strain problem of a polysilicon cylinder on a thick polysilicon substrate was analyzed. The polysilicon is modeled as linear elastic with a Young's modulus of 164 GPa, a Poisson's ratio of 0.23, and a density of 2.9 g/cm^3. The radius of

the cylinder is 25 nm. Figure 1 shows the two meshes used in the finite element analyses. At the contact point, the smallest element in the coarse mesh (1a) has a side length of 1 nm, while the smallest element in the refined mesh (1b and 1c) has a side length of 0.1 nm. The cylinder is displaced with a normal velocity of 1000 mm/s to approximate a static loading.

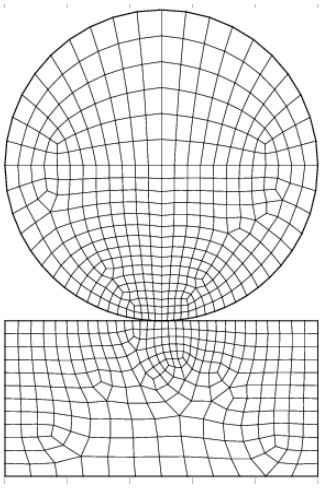

1a) Coarse mesh, smallest element side length = 1 nm.

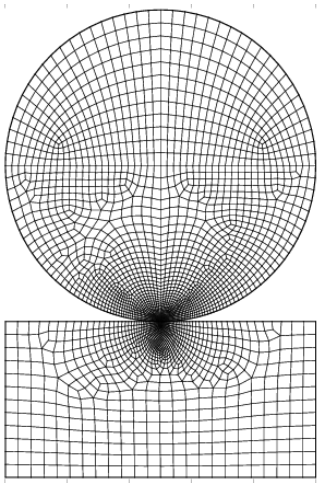

1b) Refined mesh, smallest element side length = 0.1 nm.

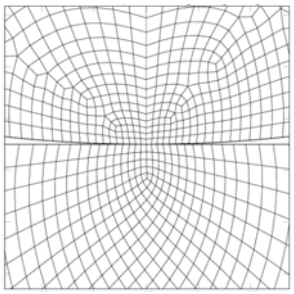

1c) Close-up view of the refined mesh at contact point.

Adhesional forces between solids are normally significant over a distance of on the order of one nm [4]. It is computationally desirable to use a minimum element size with that same length scale. However, that length scale must also be sufficient to reproduce localized contact stress. For this reason, the Hertz line contact problem was analyzed first to investigate the effect of element size on calculated contact pressure in the absence of adhesional forces. In these calculations the upper half of the cylinder is displaced downward 1 nm, generating a peak contact pressure of over 5 GPa. The calculated results are compared with the well-known analytic Hertz solution for line contacts [5] in Fig. 2. For the case of a cylinder in contact with a flat substrate of the same material,

$$\overline{p}_o = \frac{\overline{P}^{1/2}}{2} \tag{1}$$

with

$$\overline{p}_o = \frac{p_o}{E^*} \quad and \quad \overline{P} = \frac{4P}{\pi E^* R} \tag{2}$$

and where p_o is the maximum contact pressure, P is the applied line load per unit length, E is Young's modulus, ν is Poisson's ratio, R is the radius of the cylinder, and $E^* = E/(2(1-\nu^2))$. Note that the analytic solution indicates that the nondimensionalized maximum contact pressure $\overline{p}_o$ varies as the square root of the nondimensionalized applied compressive force $\overline{P}$.

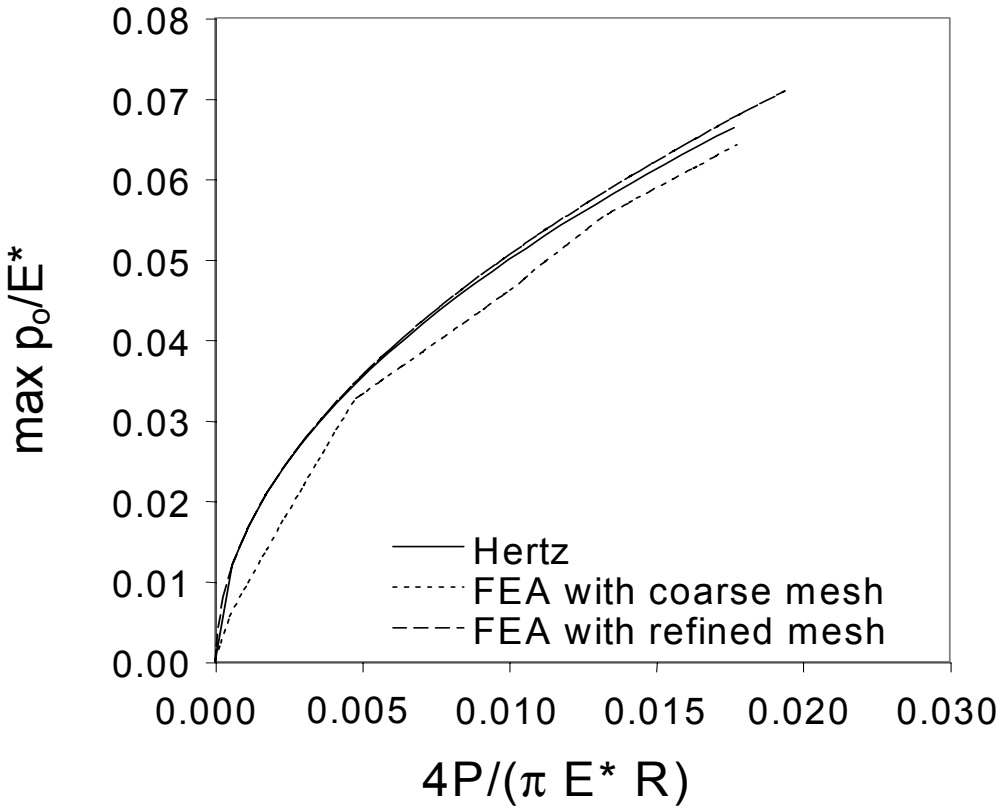

Fig. 2. Comparison of finite element (FEA) and Hertz analytic line contact solutions for a cylinder in contact with a flat substrate of the same material.

Figure 2 shows that the calculation that used the coarse mesh provides a reasonably accurate result even thought the maximum half contact width is only 3 nm (i.e. 3 element side lengths in the coarse mesh). The calculation that used the refined mesh is in very close agreement with the Hertz solution (the slight deviation from the Hertz solution at higher loads is probably a consequence of using a finite-sized substrate, Fig. 1, since at higher loads the calculated results display noticeable stress along the lower boundary of the substrate).

Next the force required to pull the 25-nm radius polysilicon cylinder off of a thick polysilicon substrate was determined as a function of the adhesion energy. To permit comparison with an available elasticity solution, the adhesional surface stress is assumed to be independent of the cross-gap distance up to a critical gap distance, beyond which surface stress vanishes (Fig. 3, the finite element calculations added finite loading and unloading slopes equal to $\sigma_0/(0.05\delta_c)$ for improved numerical stability). In the results presented below, the critical cross-gap distance, δ_c, is fixed at 1 nm, while the adhesive surface stress, σ_0, is varied to generate different levels of adhesion energy. Note, that the area under the adhesion curve equals the adhesion energy Γ_o (i.e., work of separation), and for the Fig. 3 relation, $\Gamma_o=\sigma_o\delta_c$ (e.g., Γ_o = 0.1 J/m^2 when σ_0 = 100 MPa).

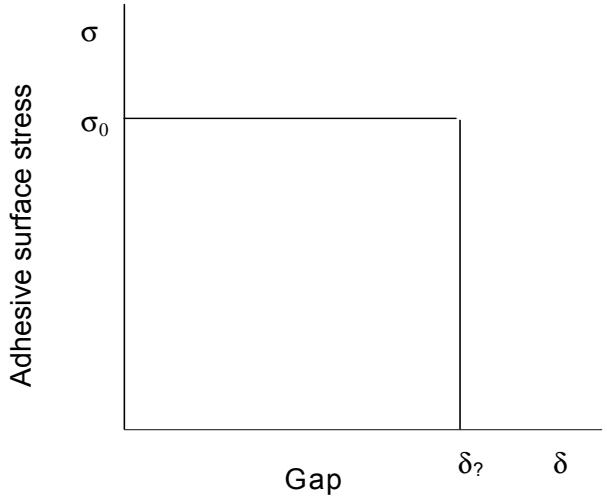

Fig. 3. Adhesion surface stress σ versus the cross-gap distance δ between surfaces.

Figure 4 plots the calculated compressive pull-off force for a range of adhesion energies. Finite element calculations were performed with both the coarse and the refined mesh (Fig. 1). These calculated results are compared with an analytic, elasticity-based solution presented in [6] (see their equation 44). The finite element results showed that for the adhesion energies considered here, there is negligible change in the polysilicon surface profiles. This suggests that the materials can be idealized as rigid, and in that case the pull-off load can be readily determined for the adhesion surface stress vs. gap distance relationship defined in Fig. 3. The length of the adhesion zone, 2b, can be determined immediately from geometric considerations.

$$b = \sqrt{2R\delta_c} \tag{3}$$

and the pull-off force/length, P, is simply equal to the adhesive surface stress σ_0 times 2b.

$$P = \sqrt{8R\Gamma_o\sigma_o} \tag{4}$$

Figure 4 shows that the elasticity-based solution and the rigid materials approximate solutions are in close agreement for the set of material parameters considered here. The calculated finite element results are within 10% of the theoretical results for a coarse mesh with a minimum element size of 1.0 nm, and are within 2% when the minimum element size was reduced to 0.1 nm.

Appendix A contains an example of the PRESTO input for the adhesion model. As an aside, note that the contact capabilities within PRESTO use a box defined around each element face to locate nodes that may potentially contact the face. This box is defined by a tolerance normal to the face and another tolerance tangential to the face. In an adhesion calculation, the normal tolerance must be set to equal to at least δ_c or the adhesion-gap relationship will be truncated. Also note that the tangential gap must be set equal to some

relatively small percent of the element side length, or the algorithm will have difficulty determining the correct node/surface pair. In the calculations presented above, the normal tolerance was set to 1.05 δ_c, and the tangential tolerance was set to 0.1 times the minimum element side length.

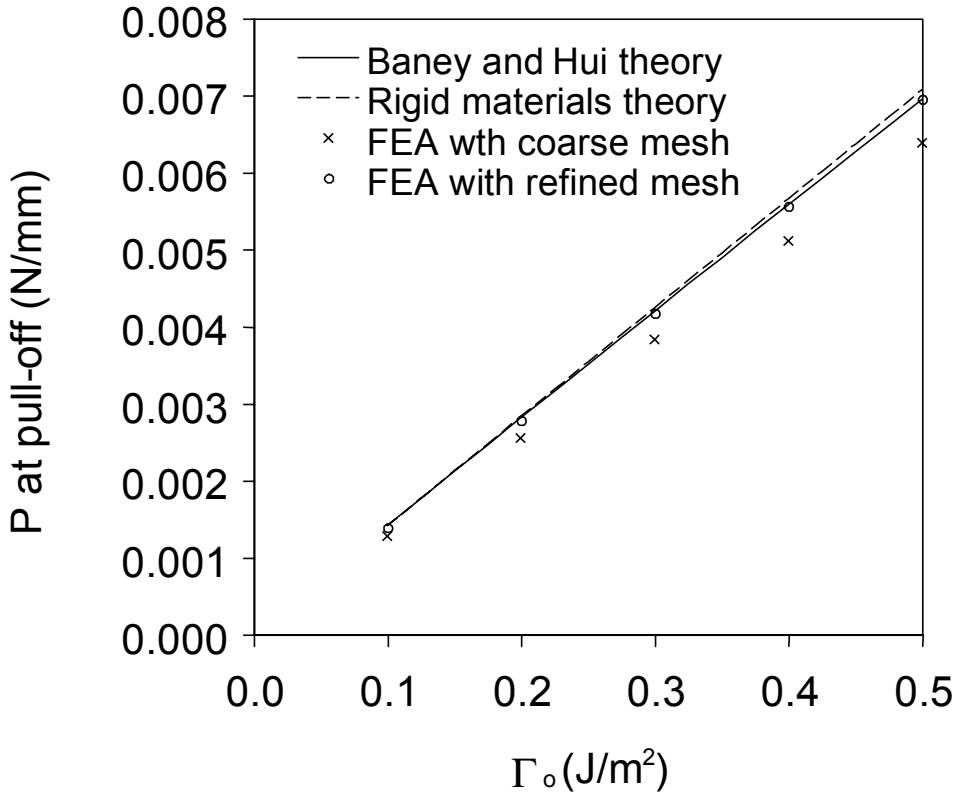

Fig. 4. Comparison of finite element (FEA) and analytic solutions for pull-off load as a function of adhesion energy.

Thin tungsten strip on a silicon substrate

In this set of calculations, a 100 nm thick tungsten layer is pulled off of a silicon substrate. A 2-D, plane strain model for a delaminated strip was analyzed to permit the comparison of the calculated results with an approximate, analytic solution for a static loading. In the calculation, one half of the strip is modeled with the symmetry condition enforced at the centerline, Fig. 5a, and the centerline nodes are displaced upward with a velocity of 10,000 mm/s (trial calculations using a 1,000 mm/s loading rate computed delamination lengths that were within 10% of these computed with a 10,000 mm/s loading rate). Elements along the interface have a side length of 5 nm. The tungsten is modeled as linear elastic with a Young's modulus of 410 GPa, a Poisson's ratio of 0.28, and a density of 19.3 g/cm^3 (the silicon properties are listed in the previous section). These calculations employed a cohesive zone (CZ) model similar to that originally formulated by Tvergaard and Hutchinson [1]. In this CZ model, the traction-separation relation is based on a potential function that depends on a scalar, effective separation.

Figure 5b shows the form of the effective traction vs. effective separation relation used in this study. The critical effective separation, defined so that the tractions drop to zero at λ=1, is fixed at 1-nm while the maximum interfacial stress $\hat{\sigma}$ is varied to generate different levels for the work of separation, G_o. Appendix B describes the model in detail and also contains an example of the PRESTO input for the CZ model ($\delta_n^c = \delta_t^c = 1nm$ in the calculations reported here).

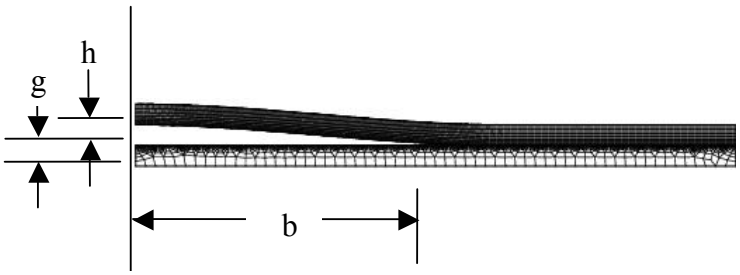

Fig. 5a. Delaminating tungsten film on a silicon substrate.

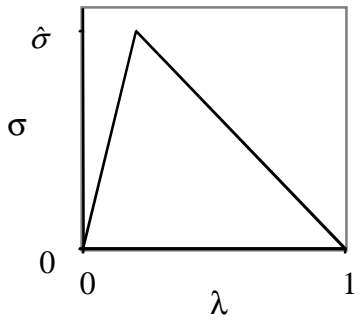

Fig. 5b. Effective traction vs. effective separation relation used in CZ model.

Figure 6 plots the calculated nondimensionalized delamination half-length, b, as a function of the nondimensionalized center deflection, g, for various values of a parameter that depends on the work of separation G_o. The calculated cohesive zone length is greater than 100 nm, which is large compared to the element size. These results are compared with an approximate analytic solution (for a static loading) that is derived using beam theory. One end of the beam is cantilevered a distance g above the substrate while the beam's other end has a zero slope at the tip of the delamination (Fig. 5a). The energy release rate per unit thickness, G, which equals to G_o for a propagating delamination, is determined using the well-known fracture mechanics relationship between G and the change in the systems potential energy with crack length (delamination half-length, b) [7]. The desired relationship is

$$b/h = (3/2)^{1/4}\left(\frac{\bar{E}h}{G_o}\right)^{1/4}\left(\frac{g}{h}\right)^{1/2} \tag{5}$$

where $\bar{E} = E/(1-\nu^2)$. Figure 6 shows that there is good agreement between the approximate, static solution and the finite element calculations.

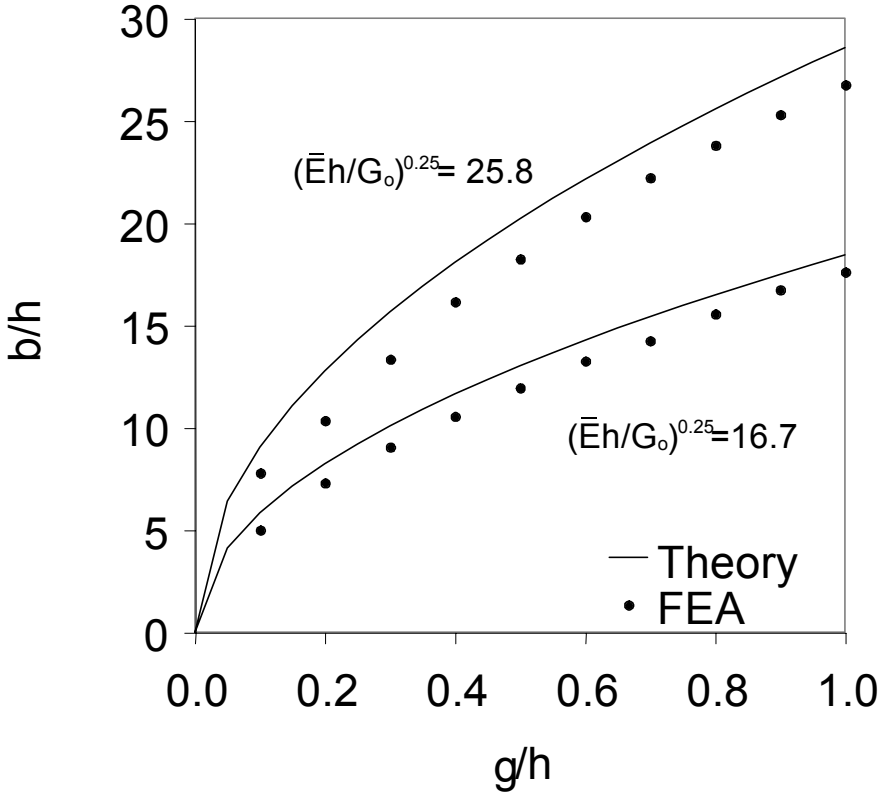

Fig. 6. Comparison of finite element (FEA) and analytic solutions for the calculated delamination half-length, b, as a function of the center deflection, g, for various values of the work of separation G_o.

Suggestions for Future Work

This one-year feasibility study has demonstrated the accuracy and usefulness of PRESTO's adhesion and cohesive zone models, and these capabilities are now available in PRESTO version 1.07. The present implementation could be made more robust by taking into account of the possibility that the adhesion and CZ models can in some circumstances control the solution's stable time step. The minimum time step used for the explicit time integration of the governing equations depends on the highest eigenvalue (vibrational mode) in the mesh. The presence of adhesion or cohesion models in the analysis can introduce or modify high frequency vibrational modes. The initial stiffness of the adhesion surface stress-gap distance relation (Fig. 3) and the traction-separation relation (Fig. 5b) determine a vibrational frequency for the connected nodes. Formulae can be derived to estimate the frequency of those vibrational modes that might impact the choice of the stable time increment. These estimates can often be based on simple idealizations that capture the main features of the mode of interest [8].

In other work, not reported above, a preliminary attempt was made to model the buckle-driven delamination of a biaxially stressed film from a substrate. Large, dynamic, transverse deflections are generated as the thin film abruptly buckles from the substrate.

Since all the materials were modeled as linear elastic in this analysis, there is no energy dissipation, and the delamination oscillates indefinitely. If one is interested in the quasi-static solution, then some form of dampening must be added. If one is interested in modeling transient response at the nano-scale, an accurate calculation must include any energy dissipation mechanisms that might exist. These mechanisms, however, are not well understood, and methods to measure nano-scale damping are a challenge.

The adhesion and cohesive zone models implemented in PRESTO are basic surface interaction models. It is likely that other surface interaction models could be formulated to give a better representation for certain situations. An initial effort was made to develop a surface interaction model that combines a novel nm-scale friction model with the adhesion model. This "junction" model was motivated by recent atomic force microscope data that suggests that the magnitude of nm-scale friction depends on the bimaterial pair's adhesion energy, but is independent of the contact stress [9]. This is undoubtedly a fruitful topic for further study.

Acknowledgements. The adhesion and cohesive zone models where implemented in PRESTO by Reese Jones (SNL/CA) and Nathan Crane (SNL/NM). This work was performed at Sandia National Laboratories. Sandia is a multiprogram laboratory operated by Sandia Corporation, a Lockheed Martin Company, for the U. S. Department of Energy under contract DE-AC04-94AL85000.

References

1. V. Tvergaard and J.W. Hutchinson, *The influence of plasticity on mixed mode interface toughness.* Journal of the Mechanics and Physics of Solids, 1993. **41**: p. 1119-1135.
2. J.R. Koteras and A.S. Gullerud, *Presto User's Guide Version 1.05 (SAND2003-1089)*. 2003, Sandia National Laboratories: Albuquerque, NM.
3. K.H. Brown, et al., *ACME: Algorithms for Contact in a Multiphysics Environment API version 1.3 (SAND2003-1470)*. 2003, Sandia National Laboratories: Albuquerque, NM.
4. J.N. Israelachvili, *Intermolecular and Surface Forces*. 2nd ed. 1992, San Diego: Academic Press.
5. K.L. Johnson, *Contact Mechanics*. 1985, Cambridge: Cambridge University Press.
6. J.M. Baney and C.Y. Hui, *A Cohesive Zone Model for the Adhesion of Cylinders.* Journal of Adhesion Science and Technology, 1997. **11**: p. 393-406.
7. M.P. de Boer and T.A. Michalske, *Accurate Method for Determining Adhesion of Cantilever Beams.* Journal of Applied Physics, 1999. **86**: p. 817-827.
8. E.D. Reedy, Jr., F.J. Mello, and T.R. Guess, *Modeling the Initiation and Growth of Delaminations in Composite Structures.* Journal of Composite Materials, 1997. **31**: p. 812-831.
9. R.W. Carpick, et al., *Making, Breaking and Sliding of Nanometer-Scale Contacts.* Material Research Society Symposium Proceedings, 1999. **539**: p. 93-103.

Appendix A

Example of PRESTO input commands used with Adhesion Model

```
 begin definition for function ADvsU
   type = piecewise linear
   ordinate = traction
   abscissa = separation
   begin values
     0.00000000       0.00
     0.00000005       1.00
     0.00000100       1.00
     0.00000105       0.00
   end values
 end definition for function ADvsU

   ### contact definition ###
   begin contact definition contact

     contact surface surface1 contains surface_2
     contact surface surface2 contains surface_11

      begin adhesion model adh
        adhesion function = ADvsU
        adhesion scale factor =100.0
      end adhesion model adh

     begin interaction inter_1
       surfaces = surface1 surface2
       automatic kinematic partition
       normal tolerance = 1.1e-6
       tangential tolerance = 0.1e-6
       friction model = adh
     end interaction inter_1
   end contact definition contact
```

Appendix B

The cohesive zone model implemented in PRESTO is the same as that used by Tvergaard and Hutchinson (they call their model the Embedded Process Zone (EPZ) model [1]). They define a cohesive potential that depends on a scalar, effective separation. The effective separation λ is expressed in terms of the normal (δ_n) and tangential (δ_t) components of the displacement difference of initially coincident points on the interface that separate as the interface fails, with

$$\lambda = \sqrt{\left(\frac{\delta_n}{\delta_n^c}\right)^2 + \left(\frac{\delta_t}{\delta_t^c}\right)^2} \tag{A1}$$

The parameters δ_n^c and δ_t^c are critical values of these displacement components and are defined so that when λ=1, the tractions drop to zero. The function σ(λ) is the effective traction vs. separation relationship and is used to define a traction potential

$$\phi(\delta_n, \delta_t) = \delta_n^c \int_0^{\lambda} \sigma(\lambda')d\lambda' \tag{A2}$$

Consequently, the normal and tangential traction components that act across the interfacial cohesive zone are

$$T_n = \frac{\partial \phi}{\partial \delta_n} = \frac{\sigma(\lambda)}{\lambda}\frac{\delta_n}{\delta_n^c} \quad \text{and} \quad T_t = \frac{\partial \phi}{\partial \delta_t} = \frac{\sigma(\lambda)}{\lambda}\frac{\delta_n^c}{\delta_t^c}\frac{\delta_t}{\delta_t^c} \tag{A3}$$

The relative contribution of shear and normal displacement (i.e., for a mixed-mode loading) is determined by specifying the value of the ratio δ_n^c / δ_t^c. Under a pure normal separation ($\delta_t = 0$), $T_n = \sigma(\lambda)$ with $\lambda = \delta_n / \delta_n^c$ and with a peak normal traction of $\hat{\sigma}$ (Fig. 5b). Under a pure tangential displacement ($\delta_n = 0$), $T_t = (\delta_n^c / \delta_t^c)\sigma(\lambda)$ with $\lambda = \delta_t / \delta_t^c$ and with a peak tangential traction of $(\delta_n^c / \delta_t^c)\hat{\sigma}$. The work of separation per unit area of interface is path independent and equals the value of the potential ϕ (eq A2) evaluated at λ = 1. Note that the formulation allows reversible behavior prior to attaining λ = 1. Also note that the PRESTO implementation constrains interfacial normal separation to prevent interpenetration when λ<1.

Example of PRESTO input commands used with Cohesive Zone Model

```
begin definition for function TvsU
  type = piecewise linear
  ordinate = traction
  abscissa = separation
  begin values
    0.0   0.00
    0.2   1.00
    1.0   0.00
  end values
end definition for function TvsU



  ### contact definition ###
  begin contact definition contact

    contact surface surface1 contains surface_2
    contact surface surface2 contains surface_13

    begin cohesive zone model czm
      critical normal gap = 0.000001
      critical tangential gap = 0.000001
      traction displacement function = TvsU
      traction displacement scale factor = 200
    end cohesive zone model czm


    begin interaction inter_1
      surfaces = surface1 surface2
      automatic kinematic partition
      normal tolerance = 1.0e-6
      tangential tolerance = 1.0e-6
      friction model = czm
    end interaction inter_1

  end contact definition contact
```

Distribution:

1	MS 0323	D. L. Chavez, LDRD office, 1011
1	MS 0824	W. L. Hermina, 9110
1	MS 0826	S. N. Kempka, 9113
1	MS 0835	K. F Alvin, 9142
1	MS 0835	N. K. Crane, 9142
1	MS 0847	A. S. Gullerud, 9142
1	MS 0847	H. S. Morgan, 9120
1	MS 0847	J. M. Redmond, 9124
1	MS 0847	M. J. Starr, 9124
1	MS 0893	P. Chaplya, 9123
1	MS 0893	J. V. Cox, 9123
1	MS 0893	D. Hammerand, 9123
1	MS 0893	M. K. Neilsen, 9123
1	MS 0893	J. Pott, 9123
10	MS 0893	E. D. Reedy, Jr., 9123
1	MS 0893	Day file, 9123
1	MS 1310	M. P. De Boer, 1762
1	MS 9161	E-P Chen, 8763
1	MS 9161	P. A. Klein, 8763
1	MS 9405	R. E. Jones, 8763
1	MS 9409	N. R. Moody, 8754
1	MS 9018	Central Technical Files, 8945-1
2	MS 0899	Technical Library, 9616